SPH-CODE KERNEL: THREE-DIMENSIONAL NUMERICAL SIMULATION OF HYPERVELOCITY PERFORATION

Vadim V. Bashurov[1], Andrei G. Ioilev[2]

[1] RFNC-VNIIEF, Mir Ave. 37, 607190 Sarov (Arzamas-16), Nizhnii Novgorod Reg., Russian Federation, E-mail: bashurov@vniief.ru

[2] RFNC-VNIIEF, Mir Ave. 37, 607190 Sarov (Arzamas-16), Nizhnii Novgorod Reg., Russian Federation, E-mail: ioilev@vniief.ru

ABSTRACT

Currently numerical modelling is used widely to evaluate the spacecraft persistence under the space debris impact. In the process of development, all the numerical codes are repeatedly tested using analytical solutions and experimental data obtained in conditions close to that of the application, to compare with. To use numerical codes for modelling of the hypervelocity impact with confidence, additional testing on problems reflecting key features associated with shielding against space debris is needed. KERNEL code based on SPH-method (*Smoothed Particles Hydrodynamics*) was developed at RFNC-VNIIEF specially for numerical simulation of three-dimensional motions of the continuous media with large deformation and fracture. Its testing using high- and hypervelocity impact experimental data showed practically full correspondence of the cavern dimensions in thick target, good agreement in dimensions of holes and fragmentation regions and reasonable agreement in geometry of the debris cloud in the case of perforation of the thin distanced sheets were obtained.

1. INTRODUCTION

Effective protection against space debris is one of key requirements to spacecraft that should keep functioning for a long period (e.g., some modules of the Space Station). Design of protection system depends strongly on possibility of prediction of spacecraft elements behaviour in the hypervelocity impact conditions. Currently numerical modelling is used widely to evaluate the spacecraft persistence under the space debris impact and during the spacecraft anti-debris shielding design. From one side, this leads to significant lowering of expenditures for experimental working-out of the structure. From the other side, this approach demands careful testing of the numerical codes.

In the process of development, all the numerical codes are repeatedly tested using analytical solutions to compare with, e.g., for well-known Noh's problem of shock-wave implosion [1] or problem of expansion of ellipsoid [2]. The codes testing with use of experimental data obtained in conditions close to that of the application, to compare with is also extremely desirable. For example, "Taylor's test" (normal impact of the solid cylinder to the rigid wall) is often used for testing of the elastic-plastic codes [3]. Aims of the test are: to check representation of free and contact boundaries under high-velocity loading (numerical method); and to check modelling of the material behaviour at large strain and high strain rate (model of material).

To use numerical codes for modelling of the hypervelocity impact with confidence, additional testing on problems reflecting key features associated with shielding against space debris [4]:

- large distance between bumpers and backwalls,
- fragmentation associated with low impact velocity or non optimum bumper thickness, double bumper configurations, oblique impacts,
- range of expected impact velocities, availability of experimental results to assess the possibilities offered by numerical simulations.

KERNEL code [5,6] based on SPH-method (*Smoothed Particles Hydrodynamics*) was developed at RFNC-VNIIEF for numerical simulation of three-dimensional motions of the continuous media with large deformation and fracture, e.g., perforation. In the process of development, the KERNEL code was tested using analytical solutions and experimental data to compare with, some results of the testing were reported in [5,6]. Validation of the KERNEL code is being performed since 1992 using experimental data on wide velocity range hypervelocity impact to semi-infinite barriers (thick targets) and multiple thin sheet barriers (of the Whipple bumper type) (see, e.g., [7,8]).

General description of the current version of the KERNEL code is presented hereinafter, as well as results of its testing using hypervelocity impact experimental data and an example of the code implementation for 3D numerical simulation of perforation of the pressure vessel wall, generation of the

Proceedings of the 3rd European Conference on Space Debris, ESOC, Darmstadt, Germany, 19 - 21 March 2001 (ESA SP-473, August 2001)

secondary debris cloud and initial phase of its evolution in gas.

1. DESCRIPTION OF CODE

Smoothed Particles Hydrodynamics (SPH) method is based on the three-dimensional free Lagrangian algorithm described for the first time in [9,10]. According to this algorithm, the media is described as spatially distributed clouds of material with the mass centres moving according to equations of the continuous media dynamics. The modelled continuous media is supposed to be described unequivocally by equations of motion, continuity and energy. The system is closed by equation of state (EOS), determining dependence of stress (or pressure) on deformation (or density) and specific internal energy. The SPH-method is based on the integral interpolation of variables stored in unordered non-regular point set. All the media is partitioned into spherically symmetrical particles spread in space with the density distribution represented by the interpolation kernel with parameter of length dimension. Initially, the SPH-method was used for astrophysics simulations only. Introducing of full strain and stress tensors' account and solving of problems with boundary conditions have made possible its implementation for numerical simulation of motions of the continuous media with large deformation [11-14].

In the KERNEL code the system of equations is solved in Cartesian co-ordinates by a solver scheme of predictor-corrector type in the following sequence [15,16]:

- begin time step;
- calculate the particles' co-ordinates;
- calculate density from equation of continuity;
- calculate velocity from equation of impulse;
- correct the particles' co-ordinates;
- calculate specific internal energy from equation of energy;
- calculate pressure from EOS;
- end time step.

The second order B-spline is used for the interpolation kernel as the best regarded for modelling of elastic-plastic flows. The "linked-list" algorithm is used to optimize calculations at searching for the nearest neighbour particles.

EOS of perfect or politropic gas is used for modelling of gases, Mie-Gruneisen or Tillotson EOS is used in modelling of solid bodies. Any other EOS in analytic or table form providing dependence of pressure on density and specific internal energy could be used. Elastic-plastic and fracture properties of materials are described by a model with variable yield and ultimate stress. Deformation or cumulative fracture criteria could be used.

Note, that numerical scheme is of the first order of accuracy in time and space, so large number of particles must be used for perfect simulation of shock wave processes.

The KERNEL code is programmed using C programming language and is working under *Microsoft Windows 98* or *Windows NT (2000)* on personal computer. A special post-processor was developed on basis of *Intel 3DR* graphic code.

Microsoft Windows NT (2000) Multi Threads options were used to parallelise the KERNEL code. This paralleling mechanism provides possibility of free access from any CPU to the whole task memory area, so every process any time can address to any element of the hydrodynamic arrays, assigned to particles. Every thread is runs at its CPU (or it is emulated, if number of processors is less than number of threads) and performs all the steps of described above predictor-corrector scheme with "its" portion of particles. Number of particles is distributed to all the threads uniformly. The calculations are synchronised at the end of time step. The semaphore mechanism is quite convenient for synchronisation: at completing calculations of a stage (e.g., stage of calculation of density) by thread, a message is generated; all threads are waiting for completion of all the calculations of the previous stage to begin calculations of the next stage (e.g., stage of calculation of velocity). Hypervelocity impact test problems simulations in 3D set-up were performed at single CPU and dual-CPU personal computers under *Windows 2000*, comparison of results obtained by parallel and sequential versions of KERNEL showed the following:

- values of "hydrodynamic" parameters in parallel and sequential calculations practically coincides;
- coefficient of paralleling is in the range of 0.81-0.875 (speedup 1.62-1.75) for real problems of perforation, it depends on number of particles and their initial location.

2. TEST PROBLEMS

2.1 Model of Metals

Mie-Gruneisen EOS with Murnaghan approximation of "cold" pressure [17,18] was used :

$$p = p_c(\rho) + \Gamma\rho E_т$$

$$E_т = E - E_c(\rho)$$

$$p_c(\rho) = \frac{\rho_0 c_0^2}{n}\left[\left(\frac{\rho}{\rho_0}\right)^n - 1\right]$$

$$E_c(\rho) = \frac{c_0^2}{n}\left[\frac{\left(\left(\frac{\rho}{\rho_0}\right)^{n-1} - 1\right)}{n-1} - 1 + \frac{\rho_0}{\rho}\right]$$

where ρ_0 is initial density, c_0 is bulk sound speed, and parameters n and Γ are matching experimental data in the pressure range of interest. Simple von Mises model with constant shear modulus G (or Poisson's ratio ν) and yield strength Y was used to model elastic-plastic properties. Simple model with Tresca type local criterion of splitting at ultimate tensile stress σ_c was used to model fracture.

2.2 Penetration of tungsten rod into steel block

Impact: normal, velocity V_0 (see Table 1), no yaw.
Projectile: rod, tungsten alloy, length l, radius r, mass m (elongation l/d≈23, see Table 1).
Target: steel block.
Comparison to experimental data [17]: post-test cavity dimensions (penetration depth L and cavity diameter D, see Table 3).

Table 1

Test #	V_0,km/s	l,cm	r,cm	m,g
1929	1.29	15.575	0.3433	100
5835	2.65	15.575	0.3380	96.96
5839	3.45	15.575	0.3376	96.73
5841	2.37	12.18	0.2638	46.20
5842	3.58	12.18	0.2633	46.02
5844	4.46	12.18	0.2615	45.41

5000 particles in projectile, 200000 particles in target were used in the solution area -200<x<200 mm, -50<y<50 mm, 0<z<50 mm for simulation. Since the problems have plane of symmetry, simulations were performed in 3D approach for a half (with rigid plane boundary at z=0). Sides of the solution area (x=200 mm; y=50 mm; z=50 mm) were modelled by "rigid wall" boundary conditions. Parameters of materials used for simulations are presented in Table 2.

Table 2

Material	Tungsten alloy	Steel
ρ_0, g/cm^3	17.78	7.81
c_0, km/s	4.612	4.9
n	3.54	4.5
Γ	1.66	1.8
G, GPa	126.615	95
Y, GPa	0.983	0.39
σ_c, GPa	-0.983	-0.39

Results of simulations and experimental data to compare are presented in Table 3. Simulated cavity dimensions are ~4% less than experimental due to yield of steel taken for guess as 0.39 GPa, since exact parameters of materials are unknown for us.

Table 3

	L,cm		D,cm	
Test #	Experiment	Simulation	Experiment	Simulation
1929	8.0	8.0	1.25	1.21
5835	22.85	22.1	1.92	1.8
5839	24.15	24.1	2.6	2.5
5841	16.52	16.1	1.3	1.25
5842	18.86	18.1	2.01	2.0
5844	19.37	19.1	2.72	2.6

2.3 Perforation of steel bumper by steel projectile

Impact: normal or oblique at angle α, velocity V_0 (see Table 4).
Projectile: spherical, steel, diameter d=13.5 mm, mass m=10 g.
Target: one bumper, steel, thickness h (see Table 4).
Comparison to experimental data [7]: x-rayograms at time t_x (see Fig.1).

Table 4

Test #	α	V_0, km/s	h, mm	t_x, mks
1	90°	3.08	2	12
3	90°	0.488	2	100
17	45°	0.908	1	25.33
20	45°	0.76	1	49.5

2000 particles in projectile, 10000 particles in target were used in the solution area -50<x<100 mm, -50<y<50 mm, 0<z<50 mm for simulation. Since the problems have plane of symmetry, simulations were performed in 3D approach for a half (with rigid plane boundary at z=0). Sides of the solution area (x=100 mm; y=±50 mm; z=50 mm) were modelled by "absorbing

boundary" conditions. Parameters of materials used for simulations are presented in Table 5.

Table 5

Material	Steel (projectile)	Steel (bumper)	Al-alloy (backwall)
ρ_0, g/cm^3	7.7	7.85	2.78
c_0, km/s	4.76	4.406	5.612
N	4	4	3.54
Γ	1.38	1.38	1.176
ν	0.3	0.275	0.362
Y, GPa	1.55	0.35	0.383
σ_c, GPa	-2.66	-0.47	-0.59

Results of simulations and experimental data to compare are presented in Fig.1. Good agreement in the projectile shape after perforation and debris number and location could be noted.

2.4 Perforation of distanced sheets by steel projectile

Impact: normal, velocity 6.2 km/s.
Projectile: spherical, steel, diameter 5.56 mm, mass 0.7 g.
Target: bumper (steel, thickness 1 mm) - gap (air, 200 mm) - backwall (aluminium alloy, 7 mm).
Comparison to experimental data [7]: high frame rate photography, post-test inspection of damage.

1000 particles in projectile, 20000 particles in bumper and 20000 particles in backwall were used in the solution area -50<x<200 mm, -120<y<120 mm, 0<z<120 mm for simulation. Since the problems have plane of symmetry, simulations were performed in 3D approach for a half (with rigid plane boundary at z=0). Sides of the solution area (x=200 mm; y=±120 mm; z=120 mm) were modelled by "rigid wall" boundary conditions. Influence of air in the gap was neglected. Parameters of materials used for simulations are presented in Table 5.

Results of simulations and experimental data to compare are presented Table 6 (damage to bumper and backwall) and Fig.2 (debris cloud at time 35 mks). Good agreement in damage to target and debris cloud could be noted.

Results of simulations and experimental data to compare are presented Table 6 (damage to bumper and backwall) and Fig.2 (debris cloud at time 35 mks). Good agreement in damage to target and debris cloud could be noted.

Table 6

Damage	Experiment	Simulation
Bumper: hole of diameter	10.5	11
Backwall:		
- max depth of crater	~4 mm (two craters in center)	~5 mm (4 craters in center)
- radius of damage area	~150 mm	~150 mm

2.5 Perforation of distanced sheets by aluminium projectile

Impact: normal, velocity V_0 (see Table 7).
Projectile: spherical, Al 2024-T3, diameter d (see Table 7).
Target: bumper (Al 2024-T3, thickness h) - gap (distance S) - backwall (Al 2024-T3, thickness H)
or
bumper 1 (Al 2024-T3, thickness h_1) - gap (distance S) - bumper 2 (Al 2024-T3, thickness h_2) - gap (distance S) - backwall (Al 2024-T3, thickness H) (see Table 8).
Comparison to experimental data [4]: post-test inspection of damage.

2000 particles in projectile, 10000 particles in bumpers and 10000-30000 particles in backwall were used in the solution area -50<x<200 mm, -100<y<100 mm, 0<z<100 mm for simulation. Since the problems have plane of symmetry, simulations were performed in 3D approach for a half (with rigid plane boundary at z=0). Sides of the solution area (x=200 mm; y=±100 mm; z=100 mm) were modelled by "rigid wall" boundary conditions. Parameters of Al 2024-T3 used for simulations are presented in Table 5 (aluminium alloy).

Results of simulations and experimental data to compare are presented Table 7 (damage to bumpers and backwall), good agreement could be noted.

Table 7

Test	Experiment	Simulation
W.P.1 V_0=6.5 km/s d=5 mm h=1.5 mm S=200 mm H=1.5 mm	Bumper: hole diameter 11.5 mm Backwall: no perforation, main impact area 130 mm diameter, bulging, localized spalls on external crater ring	Bumper: hole diameter 11 mm; Mean velocity of the debris cloud 2.5-3.5 km/s. Backwall: no perforation, numerous damage area 120 mm diameter, bulging.
W.P.2 V_0=3.1 km/s d=10 mm h=2 mm S=200 mm H=10 mm	Bumper: hole diameter 17 mm Backwall: no perforation, extensive bulging and spalls, largest crater depth 6 mm.	Bumper: hole diameter 16 mm Mean velocity of the debris cloud 2.0-2.2 km/s. Backwall: no perforation, numerous damage area 150 mm diameter, bulging.
W.P.3 V_0=8 km/s d=4 mm h_1=0.8 mm h_2=0.5 mm S=60 mm H=3.2 mm	Bumper 1: hole diameter 7.8 mm, main half spray angle 30°, debris cloud velocity behind bumper 1: 6.76 km/s; Bumper 2: petalled hole diameter ~70 mm, main half spray angle 14°, debris cloud velocity behind bumper 2: 0.975 km/s; Backwall: peak pressure 6.1 kbar (center).	Bumper 1: hole diameter 7.5 mm Mean velocity of the debris cloud ~6 km/s, main half spray angle 35° Bumper 2: petalled hole diameter 51 mm Mean velocity of the debris cloud ~0.9 km/s, main half spray angle 15° Backwall: no perforation, numerous damage area >160 mm diameter

3. SIMULATION OF HYPERVELOCITY IMPACT TO PRESSURE VESSEL

Special study was performed at Ernst-Mach-Institute (Germany) to clear deceleration of debris in gas and generation of shock wave in gas after perforation of the PV front wall by hypervelocity projectile [20-22]. In parallel to the experimental study, numerical simulations of the PV front wall hypervelocity perforation and generation of debris cloud with initial phase of generation of shock wave in gas were performed [22]. The simulations were performed using AUTODYN-2D SPH-code [23] in 2D axis-symmetrical set-up: normal impact of Al sphere 5 mm diameter at 5.2 km/s to unshielded 1.5 mm Al wall of PV containing nitrogen under pressure of 0.1 and 10.5 bar. Comparison to the experimental data (high frame rate photography) showed good agreement along center line (formation of central residual large fragment and a shock wave gas flow about it during flight) and qualitative correspondence in formation and flight of lateral fragments generating lateral shock wave in gas. All the fragments are really separate particles, and this is not actually reproduced in 2D axis-symmetrical simulations, thus leading to discrepancy in shock wave flow. To estimate influence of 3D effects on modelling, 3D numerical simulation was performed using KERNEL.

Geometrical set-up of KERNEL simulations corresponds to that of AUTODYN-2D [22]: normal impact of Al spherical projectile 5 mm in diameter at 5.2 km/s to vessel containing gas (nitrogen). The vessel front wall (subjected to impact) is 1.5 mm thick and made of Al-alloy Al 5754. Influence of air at ambient conditions outside the vessel (from the impact side) was neglected. Nitrogen under pressure of 10.5 bar is inside the vessel.

2000 particles in projectile, 20000 particles in front wall and 150000 particles in gas were used in the solution area $-50<x<150$ mm, $-120<y<120$ mm, $0<z<120$ mm for simulation. Since the problems have plane of symmetry, simulations were performed for half in 3D approach with rigid plane boundary at z=0. Sides of the solution area (x=150 mm; y=±120 mm; z=120 mm) were distanced enough to neglect their influence on the debris flight and shock wave propagation during the simulations, so they were modelled by "rigid wall" boundary conditions. Ablation of debris was neglected. Parameters of projectile and bumper materials used for simulations are presented in Table 8. Perfect gas equation of state with Poisson adiabatic exponent γ=1.4 was used to model nitrogen, density 13.125 kg/m^3 corresponds to initial pressure 10.5 bar (specific internal energy is 0.2 kJ/g).

Results of 3D simulations by KERNEL code are presented in Fig.3, results of experiments and 2D simulations by AUTODYN-2D code [22] are presented also for comparison. Note, that initial phase of expansion of the secondary debris cloud in gas is reproduced well, even with taken rather small number of particles.

Table 8

Material	Al-alloy (projectile)	Al-alloy (bumper)
ρ_0, g/cm^3	2.701	2.78
c_0, km/s	5.24	5.612
N	3.54	3.54
Γ	0.97	1.176
ν	0.33	0.362
Y, GPa	0.075	0.383
σ_c, GPa	-0.1	-0.59

4. CONCLUSION

Comparison to published experimental data on high- and hypervelocity impact at velocity of 0.5-8 km/s have shown, that 3D simulations performed with the KERNEL code even using simple model of material (Mie-Gruneisen EOS with Murnaghan approximation of "cold" pressure, von Mises model with constant shear modulus and yield, Tresca type local criterion of splitting at ultimate tensile stress) provides:

- good prediction of damage (piercing and cratering) caused by large particles (initial projectile and large fragments of debris cloud);
- reasonable description of the debris cloud geometry (in the case of perforation of the thin sheets).

Ways to better correspondence are obviously the following:

- increase number of particles,
- use more precise EOS with effects of melting and evaporation of material,
- use sophisticated models for fracture of solid material and behaviour of fractured material.

In future simulations will be performed with these enhancements. However, this implies higher requirements on computer system to keep reasonable run-time. Since the main damage (piercing and cratering) is caused by large particles, and small particles of the debris cloud produce mainly spreaded pulsed loading, in many cases demonstrated usual approach is sufficient to assess survivability of structure under hypervelocity impact.

Significant portion of space debris at practically important orbits have velocity more than 8 km/s relative to spacecraft (for ISS in the range 8-12 km/s, see, e.g., [24]). So, it is necessary to continue development of the spacecraft structure material models suitable for conditions of hypervelocity impact in the velocity range 8-12 km/s (including determination of parameters) and testing of numerical codes. Currently, some experimental data on hypervelocity perforation in this velocity range are available now (see, e.g., [25,26]), but, unfortunately, they are not suitable for verification of numerical codes, because projectile in these "record" experiments was formed by shaped charge [26-28], with the help of special orifice at the light gas gun muzzle [29], or in multi-stage explosive accelerator [30,31], its shape (and mass) and orientation are not yet reproduced with sufficient stability.

Implementation of KERNEL code for 3D numerical simulation of perforation of the pressure vessel wall, generation of the secondary debris cloud and initial phase of its evolution in gas, provided good correspondence to obtained at Ernst-Mach-Institute experimental data on parameters of the secondary debris cloud.

Acknowledgements- Thanks to Frank Schaefer and Stefan Hiermaier for kind permission to use their data for comparison. The work was performed under partial funding by ISTC Project # 1334.

5. REFERENCES

1. Noh W.F., Errors for Calculations of Strong Shocks Using an Artificial Viscosity and an Artificial Heat Flux, *J. Comput. Phys.*, Vol.**72**, 78, 1987.

2. Nemchinov I.V., Expansion of Triaxial Gas Ellipsoid in Regular Mode, *Soviet Appl. Math. Mech.*, No.1, 134-140, 1964.

3. Johnson G.R., Colby D.D., Vavrick D.J., Three-Dimensional Computer Code for Dynamic Response of Solids to Intense Impulsive Loads, *Int. J. Num. Methods Engng.*, Vol.**14**, 1865-1871, 1979.

4. Lambert M., Hydrocodes, *IADC Meeting*, Houston, Dec.9-12, 1997.

5. Bashurov V.V., SPH Code for Modelling 3D Elastic-Plastic Flows Using Smoothed Particles Method. *Int. Workshop on New Models and Numerical Codes for Shock Wave Processes in Condensed Media*, St.Peterburg, Russia, Oct.9-13, 1995.

6. Bashurov V.V., Patynina A.V., Numerical Smoothed Particles Method in Three-dimensional Approach for Modelling of Physical Processes: Example of Impact and Perforation Problems, VANT, Ser. Math. Modelling of Physical Processes, No.1, 26-38, 1999.

7. Bashurov V.V., Bebenin, G.V., Belov, G.V., et al. Experimental Modelling and Numerical Simulation of High- and Hypervelocity Space Debris Impact to Spacecraft Shield Protection, *Int. J. Impact Engng.*, Vol.**20**, 69-78, 1997.

10. Ioilev A.G., Bashurov V.V., and Patyanina A.V., Advanced Numerical Simulations For Hypervelocity Impact: ESA Benchmark Simulations Using KERNEL Code, *IADC Meeting*, Darmstadt, Oct.11-13, 1999.

11. Gingold R.A., Monaghan J.J., Smoothed Particle Hydrodynamics: Theory and Applications to Non-Spherical Stars. *Month. Not. Royal Astr. Soc.*, Vol.**181**, 375-389, 1977.

12. Lucy L.B., A Numerical Approach to the Testing of the Fission Hypothesis, *Astron. J.*, Vol.**83**, 1013, 1977.

13. Cloutman L.D., An Evaluation of Smoothed Particle Hydrodynamics, *Advances In the Free-Lagrange Method.* Lecture Notes on Physics, Vol.**395**, 248-266, 1990.

14. LiberskyL.D., and Petschek A.G., Smoothed Particle Hydrodynamics with Strength of Materials, *Advances In the Free-Lagrange Method.* Lecture Notes on Physics, Vol.**395**, 267-294, 1990.

15. Libersky L.D., Petschek A.G., Carney T.C., Hipp J.P., and Allahbadi F.A., High-strain Lagrangian Hydrodynamics. A Three-dimensional SPH Code for Dynamic Material Response, *J. Comput. Phys.*, Vol.**109**, 67-75, 1993.

16. LiberskyL.D., and Petschek A.G., Cylindrical smoothed particle hydrodynamics, *J. Comput. Phys.*, **109**, 76-83, 1993.

17. Zel'dovich Ya.B., and Raizer Yu.P., *Physics of Shock Waves and High Temperature Hydrodynamic Phenomena.* Moscow, Science Publ. (1966).

18. Murnaghan F.D., *Proc.Nat.Acad.Sci.*, Vol.**30**, 244-248, 1944.

19. Silsby G.F., Penetration of Semi-infinite Steel Targets by Tungsten Rods at 1.3 to 4.5 km/s, *Proc. VIII Int. Symp. Ballistics*, Orlando, 1984.

20. Schaefer F.K., Schneider E.E, Lambert M., and Mayseless M., Propagation of Hypervelocity Impact Fragment Clouds in Pressure Gas, *Int. J. Impact Engng.*, Vol.**20**, 697-710, 1997.

21. Telichev I.Ye., Schaefer F.K., Schneider E.E, and Lambert M., Analysis of the Fracture of Gas-filled Pressure Vessels under Hypervelocity Impact, *Int. J. Impact Engng.*, Vol.**23**, 905-919, 1999.

22. Hiermaier S., and Schaefer F.K., Hypervelocity Impact Fragment Clouds in High Pressure Gas Numerical and Experimental Investigations, *Int. J. Impact Engng.*, Vol.**23**, 391-400, 1999.

23. Hayhurst C.J., and Clegg R.A., Cylindrically Symmetric SPH Simulations of Hypervelocity Impacts on Thin Plates" *Int. J. Impact Engng.*, Vol.**20**, 337-348, 1997.

24. Nazarenko A.I., Technique and Some Results of Space Debris penetration Probability Estimates for Russian Modules of ISS, *IADC Meeting*, Darmstadt, October 11-13, 1999.

25. Christiansen E.L., and Kerr J.H., Projectile Shape Effects on Shielding performance at 7 km/s and 11 km/s. *Int. J. Impact Engng.*, Vol.**20**, 165-175, 1997.

26. Bol J., and Fucke W., Shaped Charge Technique for Hypervelocity Impact Tests at 11 km/s on Space Debris Protection Shield, *Proc. 2nd European Conf. Space Debris*, Darmstadt, March 17-19, 1997, **ESA SP-393**, 405-411.

27. Walker J.D., Grosch D.J., and Mullin S.A., A Hypervelocity Fragment Launcher Based on an Inhibited Shaped Charge, *Int. J. Impact Engng.*, Vol.**14**, 763-774, 1993.

28. Katayama M., Takeba A., Toda S., and Kibe S., Analysis of Jet Formation and Penetration by Conical Shaped Charge with the Inhibitor, *Int. J. Impact Engng.*, Vol.**23**, 443-454, 1999.

29. Chhabildas L.C., Kmetyk L.N., Reinhart W.D., and Hall C.A., Launch Capabilities to 16 km/s, *Shock Waves in Condensed Matter*, Pt.2, 1197-1200, 1995.

30. Bat'kov Yu.V., Kovalev N.P., Kovtun A.D., et al., Explosive Three-Stage Launcher to Accelerate Metal Plates to Velocities More Than 10 km/s, *Int. J. Impact Engng.*, Vol.**20**, 89-92, 1997.

Fig.2. Debris cloud after perforation of steel sheet by steel spherical projectile: experimental shadowgraph (left) and results of simulations (right)

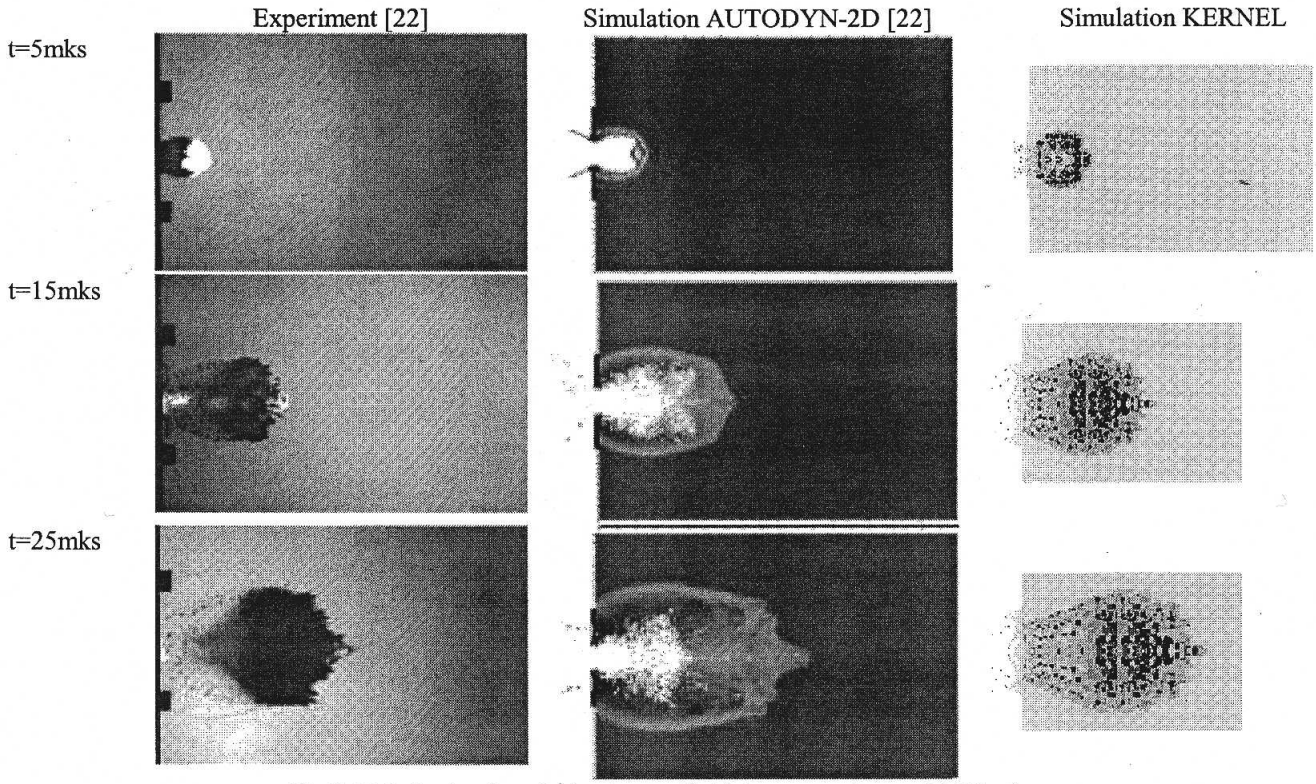

Fig.3. Debris cloud evolution in gas (initial pressure in gas 10.5 bar)

31. Geille A., Status of Development of Space Debris Hypervelocity Explosive Multi-Stage Launcher, *Int. J. Impact Engng.*, Vol.**20**, 271-280, 1997.

Test #1

Test #3

Test #17

Test #20

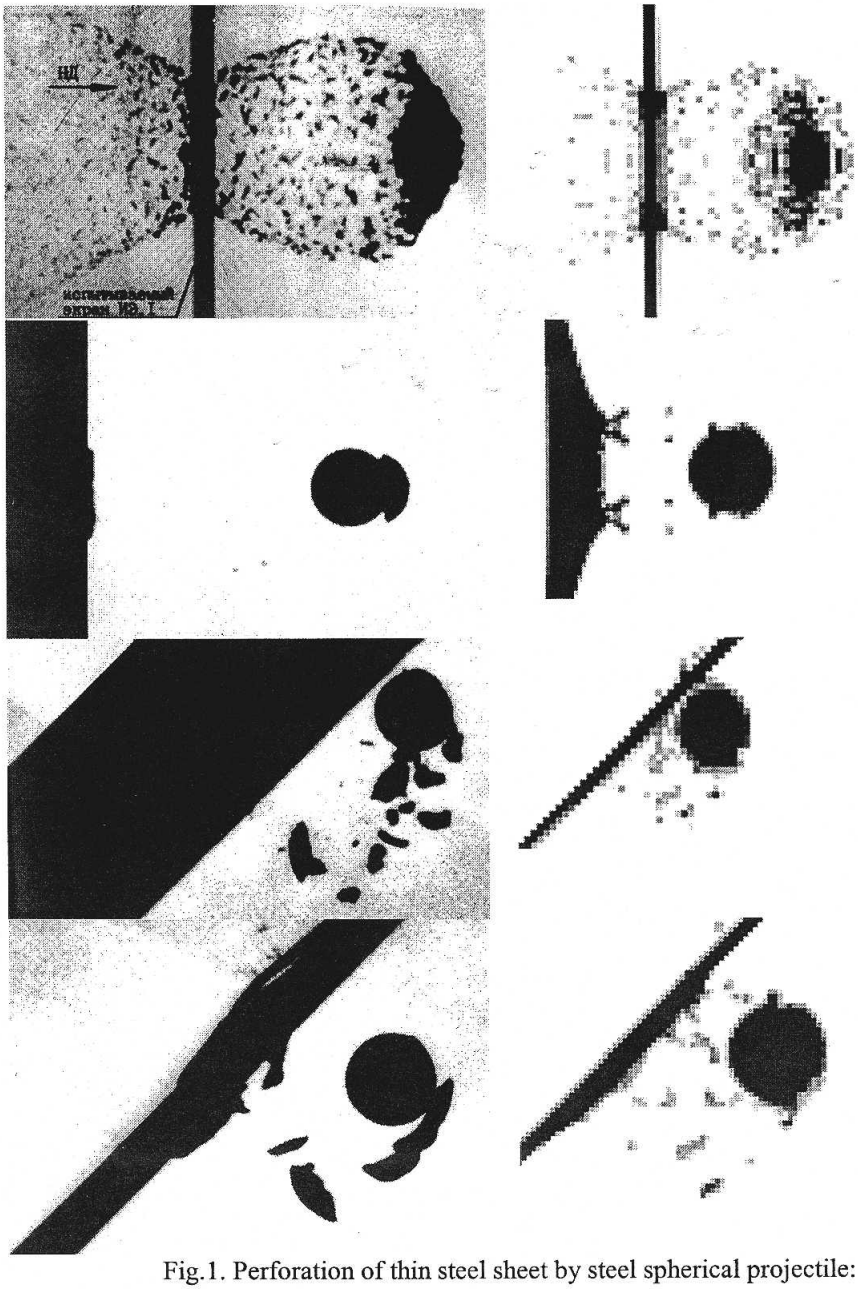

Fig.1. Perforation of thin steel sheet by steel spherical projectile: experimental x-rayograms (left) and results of simulations (right)